PB 201 620

OPTIMIZATION OF A SIMPLE DYNAMIC MODEL OF A RAILROAD CAR UNDER RANDOM AND SINUSOIDAL INPUTS

By John S. Mixson and Roy Steiner

NASA Langley Research Center
Langley Station, Hampton, Va.

Presented at the ASME Annual Meeting - "Symposium on Random Processes in Dynamical Problems"

Los Angeles, Calif.
November 16-21, 1969

40

[redacted]

03 - Rail Vehicles & Components

TECHNICAL REPORT STANDARD TITLE PAGE

1. Report No.	2. Government Accession No.	3. Recipient's Catalog No.
FRA-RT-72-04		

4. Title and Subtitle
Optimization of a Simple Dynamic Model of a Railroad Car under Random and Sinusoidal Inputs

5. Report Date
November 16-21, 1969

6. Performing Organization Code

7. Author(s)
John S. Mixson
Roy Steiner

8. Performing Organization Report No.

9. Performing Organization Name and Address
NASA Langley Research Center
Langley Station
Hampton, Virginia

10. Work Unit No.

11. Contract or Grant No.

12. Sponsoring Agency Name and Address

13. Type of Report and Period Covered

14. Sponsoring Agency Code

15. Supplementary Notes

16. Abstract

~~This~~ investigation was concerned with techniques for determining values of damping and spring constants that would minimize the vibrations transmitted from irregular railroad track to passenger positions. Results developed for a three-degree-of-freedom model using a simplified representation of measured track roughness illustrate the influence on the minimizing values of the type of input used, the minimization criteria adopted, and the position at which vibrations were minimized. The results were sensitive to variations of the spectrum of the input, suggesting the importance of measuring actual track irregularities and of using the measured data in optimization studies. Different results were obtained when the rms acceleration was minimized than when peak value of spectral density was minimized, suggesting that the effects on passenger comfort of overall accelration level be compared with the effect of vibrations that are concentrated near a single frequency. Results obtained by varying the suspension stiffness of a heavy electrical transformer suspended beneath the center of the particular type of railroad car suggest that such heavy components can be tuned to improve the vibration transmission characteristics of the system.

17. Key Words
dynamic model
simulation
vibration response
track roughness
ride quality
high-speed railroads

18. Distribution Statement
Distribution is unlimited. Copies of this report may be purchased from the National Technical Information Service, Springfield, Virginia 22151.

19. Security Classif. (of this report)	20. Security Classif. (of this page)	21. No. of Pages	22. Price

Form DOT F 1700.7 (8-69)

OPTIMIZATION OF A SIMPLE DYNAMIC MODEL OF A RAILROAD CAR UNDER RANDOM AND SINUSOIDAL INPUTS

By John S. Mixson and Roy Steiner

ABSTRACT

This investigation was concerned with techniques for determining values of damping and spring constants that would minimize the vibrations transmitted from irregular railroad track to passenger positions. Results developed for a three-degree-of-freedom model using a simplified representation of measured track roughness illustrate the influence on the minimizing values of the type of input used, the minimization criteria adopted, and the position at which vibrations were minimized. The results were sensitive to variations of the spectrum of the input, suggesting the importance of measuring actual track irregularities and of using the measured data in optimization studies. Different results were obtained when the rms acceleration was minimized than when peak value of spectral density was minimized, suggesting that the effects on passenger comfort of overall acceleration level be compared with the effect of vibrations that are concentrated near a single frequency. Results obtained by varying the suspension stiffness of a heavy electrical transformer suspended beneath the center of the particular type of railroad car suggest that such heavy components can be tuned to improve the vibration transmission characteristics of the system.

OPTIMIZATION OF A SIMPLE DYNAMIC MODEL OF A RAILROAD CAR UNDER RANDOM AND SINUSOIDAL INPUTS

By John S. Mixson and Roy Steiner

INTRODUCTION

The recent introduction of high-speed railroad passenger service between Washington, D. C. and New York has stimulated considerable interest in the effects of vibration on passenger comfort. For example, a recent newspaper account (reference 1) describes the high-speed Metroliner train, shown in figure 1, as "smooth riding," but also says ". . . at times the train vibrated badly during a 114 mph run between Washington and Baltimore, making it hard for passengers to read." Clearly, if the desired speeds of 160 mph (reference 2) are to be practical, methods must be developed for preventing such passenger discomfort due to train vibrations. Efforts are now underway in a number of organizations, including Langley Research Center, to improve the understanding of the mechanisms of transmission of vibrations to passengers, and to determine the limits of vibration for comfort. The primary source of train vibrations is the roughness of the track and roadbed so efforts are also underway to determine methods of measuring and improving track/roadbed properties.

Some of the research that has been done related to vehicle and roadbed dynamics is reported in references 3 through 9. In reference 3 a frequency domain technique for calculating response is compared with time domain techniques and found to be somewhat more efficient for linear systems having random inputs that are statistically stationary. In reference 4 the influence of roadbed elasticity is studied; and in reference 5 the dynamic stresses in railroad wheels are studied. In reference 6 a dynamic model having many degrees of freedom is described, along with a system for measuring track roughness. References 7 and 8 provide additional information on techniques for identifying roadbed properties. In reference 9 some techniques for minimizing the dynamic response of a vehicle are developed. A topic not sufficiently discussed in the literature is that of minimizing the dynamic response of rail vehicles by appropriate adjustment of the vehicle damping and spring constants.

The investigation described in this paper represents an attempt to obtain understanding of the significant parameters involved in minimizing the vibrations transmitted from the track to the passenger positions. It is known that the response of a dynamic system such as a railroad car can be minimized by choosing certain (optimum) values of the damping elements in the system. The objective of the present investigation was to determine the influence on the optimum values of damping of such things as the nature of the input (sine or random), the optimization criteria, and the location at which the vibration is optimized. The particular railroad car studied had a heavy electrical transformer suspended beneath the center of the car, so the spring stiffness of the transformer suspension was also varied in an attempt to minimize the car response. In order to keep the computations from becoming unwieldy only three degrees of freedom were included in the mathematical model, and a simplified representation of the track roughness spectrum was used. The plan of this paper is to discuss first the analysis and optimization procedure (leaving the equations for an appendix), then to discuss the track roughness measurements, and finally to discuss the results obtained with the three degree of freedom model.

ANALYSIS

A sketch of the three-degree-of-freedom model used in this analysis is shown in figure 2. The equations of motion of this system are presented in Appendix B. The model consists of a flexible beam representing the railroad car, and a mass attached at the midpoint of the beam representing an electrical transformer used in the power system of these particular electrically driven high speed trains. The degrees of freedom considered are rigid body vertical motion of the car and of the transformer and the first elastic bending mode of the car. The input to this system is provided by the specified motion of the base. The base vibrates symmetrically, thereby applying the same displacement to the lower ends of both springs k_s and both dampers c_s. Pitching and lateral motion are not included in this analysis.

The parameters held constant throughout this analysis include the weights of the car and transformer and the car rigid body and bending frequencies. The values used, shown in figure 2, were felt to be reasonably representative of current designs. The three parameters varied in the search for an optimum design are the transformer frequency f_g, the car damping n_s (due to C_s), and the transformer damping n_g (due to C_g). Optimization was carried out with respect to accelerations calculated for three locations; the end of the car $A(0)$, the center of the car $A(L/2)$, and the transformer $A(G)$.

OPTIMIZATION PROCEDURE

The general objective of the optimization was to minimize the accelerations at the two car locations caused by a specified displacement of the vibrating base. Two minimization methods were used. The first method, called the peak minimization method, minimizes the maximum value of the acceleration transfer function (for sine input) or spectral density (for random input) occurring anywhere in the frequency range of interest. The second method, called the RMS method, minimizes the root-mean-square acceleration obtained by integrating over the frequency range of interest. The peak min. method was used with both sine and random input displacements, but the RMS method was used only for random inputs.

The procedure used in the peak min. method with a sinusoidal input is as follows. First, acceleration transfer functions for the three locations were generated for the frequency range from 0 to 15 cps. Typical transfer functions (also the optimum) are shown in figure 3. The transfer function for each location has relative maximums, or peaks, at about 1 cps, and 4.5 cps. For the two car locations a third peak occurs at about 5.5 cps. The value of each transfer function at each peak is clearly dependent upon the particular values of damping, n_g and n_s, and transformer frequency f_g used to generate the transfer function. The next step in the optimization procedure was to generate curves such as shown in figure 3 for several values of one of the parameters n_g, n_s or f_g while holding other parameters constant. The value of the transfer function at each peak is then plotted as a function of the varying parameter. Typical curves of this type are shown in figure 4, where the varying parameter is the transformer frequency. The peaks of the transfer functions occurred near 1, 4.5 and 5.5 cps for all the parameter variations, therefore these frequency values were used as a convenient means of identifying the curve shown in figure 4 associated with each peak. Each curve showing the variation of a peak value of the acceleration transfer function with a varying parameter (in figure 4, the transformer frequency) is called a peak acceleration curve. Figure 4 shows that there are three peak acceleration curves for each location. An acceleration maximum function is now defined as that function consisting of the largest of the peak acceleration curves for each value of the varying parameter. The acceleration maximum function for each location shown in figure 4 consists of the segments of the peak acceleration curves joining the circular symbols. The next optimization step consists of choosing a value of the varying parameter that minimizes the acceleration maximum functions. Figure 4 shows that the transformer frequency value of 4.7 cps minimizes the maximum function for both car locations, but not for the transformer. In general, the transformer maximum function could not be minimized along with those at the car locations. Further discussion of the choice of optimum values is presented in "Results." The next step in the optimization was to use the minimizing value of transformer frequency (obtained from plots such as shown in figure 4) as a constant while varying a second parameter. Peak acceleration curves obtained by varying transformer damping are shown in figure 5, and those obtained by varying car damping are shown in figure 6. The steps described above were repeated until the parameter value obtained as optimum was sufficiently close to the value used in the previous minimization cycle. The curves shown in figures 4, 5, and 6 are from the final iteration cycle from which the optimum values were determined for the sinusoidal input. Figures 4, 5, and 6 will be discussed further under "Results."

The optimization procedure used in the peak min. method with a random input is the same as with a sinusoidal input, except that peak values were obtained from curves of spectral density of the output acceleration instead of from curves of transfer function. Spectral density maximum function is defined as consisting of the largest of the peak spectral density curves at each value of the varying parameter. For the model characteristics of this study three optimization cycles, or iterations, were sufficient, that is, each of the parameters n_s, n_g and f_g was varied three times with improved values of the other two parameters. Even with only three cycles required for each of three parameters considerable time was spent generating and plotting data to obtain the results presented herein. If many more than three parameters were to be optimized, this procedure would probably require improved computer mechanization in order to be used efficiently. An example of the use of computer techniques in an optimization procedure is given in reference 9.

The optimization procedure used in the RMS method with the random displacement input is as follows. Values of the root-mean-square (rms) acceleration at each of the three locations are calculated by means of equation (B7) for a range of values of one of the parameters n_s, n_g or f_g while all other parameters are held constant. A value of that one parameter is then chosen so that the rms acceleration at the car locations is reduced as much as possible. The value chosen is then held constant while a second parameter is varied.

Optimum values of the parameters f_g, n_g, and n_s were obtained from only a few cycles of iteration using this method.

TRACK ROUGHNESS MEASUREMENTS

General

The input for the mathematical model to describe the response of the railroad car is some measurement of the rail surface. This input is generally considered to be random in nature and takes the form of a power spectral density of the rail displacements or vertical variations from some datum plane. Spectral densities of several different types of surfaces, artificially prepared, are shown in figure 7 plotted against wave length in feet and a spatial frequency in cycles per foot. Disregarding the curve for the railroad in the eastern United States for the present, the remaining curves from reference 4 for a highway, three airport runways and a British railroad give a rather orderly group of spectra. Figure 7 indicates that the spectra from the several surfaces can be represented generally by the formula

$$\phi(f) = Kf^{-n}$$

where f is the frequency, n is the parameter determining the variation of $\phi(f)$ with the frequency, and K is a constant for a given spectrum and is a measure of the surface roughness. It is apparent from figure 7 that the exponent n which determines the slope of the spectra is fairly uniform. For these examples n varies from 2.0 to 4.1.

Two spectra were selected for use in this analysis having slopes or n values of 2.07 and 2.64 and are shown in figure 8 plotted against cycles per second. It is not considered necessary that the root-mean-square values agree precisely with experimental results in this analysis since an examination of equations B6 and B7 in appendix B indicates that the rms value is a constant and would not affect the relative magnitudes of the peaks of the spectra of the response. The rms value is a measure of the intensity of a spectrum and is equal to the square root of the area under the spectrum.

Experimental Spectrum

Available measurements of a two mile section of track in the eastern United States were analyzed at LRC and the resulting spectrum is shown in figures 7 and 8 for comparison with the spectra used in the analyses. It is apparent from figure 7 that this measured spectrum falls within the grouping of spectra and gives added confidence in the spectra used in the analysis. The spectrum for the railroad in the eastern U. S. does not, however, necessarily indicate a uniform slope. In addition, three peaks are rather prominent at 40, 20 and 14 foot wave lengths. These wave lengths correspond to the rail lengths, the spacing of alternate joints of the two rails, and the length of the rod in the rail—roughness measuring system. These relations may be coincidental, but the results can point out the care which must be exercised in the measurement, analysis, and interpretation of experimental spectra. There is always the possibility that the recording system or the data analysis technique may contaminate the results. Let us consider briefly the measurement of track roughness and data evaluation.

Measurement of Track Roughness

It is necessary to devise methods of measuring the track displacements under dynamic conditions since the elastic track moves under normal usage due to such parameters as the train weight, spacing of the ties, irregularities in the roadbed, and the impact loads due to the train movement. Most current rail measuring devices are variations of a three point measuring device such as the one in use by Melpar (reference 6). The system consists of two horizontal rods suspended from the axle of the railroad car, one rod parallel to each track. Each rod has three capacitance transducers mounted on it. The output of each transducer is related to its distance from the rail and suitable combination of the transducer outputs yields a reading related to the shape or roughness of the railroad track. These readings were recorded continuously for several stretches of track and the continuous readings were digitized for spectral analysis. The spectrum for a large range of wave lengths cannot be defined because a filter in the form of the rod length used in the measurement has been inserted in the system. In the system described, the rod length was 14 feet and the spectral analysis will yield fairly good estimates of the spectrum for wave lengths between approximately 9 and 28 feet. The effect of this filter on the spectrum was investigated analytically and corrections were applied to the spectrum. The adjusted spectrum is shown in figures 7 and 8 over a wave length range of 9 to approximately 150 feet.

In further mathematical studies of train dynamics, better measured spectra of track roughness should be obtained accurately at frequencies down to about 0.1 cps as an input to the studies. Significant problems may be encountered in trying to get data at these low frequencies as indicated by the preceding discussion. One procedure which may be used to establish the spectral shape and then the relative roughnesses (K value) is outlined:

1. Survey a two-mile section of the track in the static unloaded condition to establish the shape of the railway roughness spectrum.

2. Repeat survey with the track loaded (train advances as the survey advances) to determine constancy of spectral shape and railway roughness.

3. Determine roughness under dynamic conditions with car-mounted equipment for several speeds. (Constant monitoring required with adjustment in procedures as indicated by results)

4. With spectral shape and intensity of railway roughness established, calibrate other types of measuring equipment if compatibility of all data is desired.

5. Repeat procedure on at least two additional tracks to determine the variations of spectral shapes.

Factors in Evaluation of Power Spectra

Data analysis may be based on digital or analog techniques. In the analysis of terrain roughness and low frequency data, such as atmospheric turbulence, it has been customary to use a digital procedure. The extent of the alterations and the statistical reliability of the spectral estimates resulting from a digital technique are indicated in reference 10 and considered in greater detail in reference 11. Three important factors in defining the accuracy of the spectral estimates are the record length, the reading interval and the number of estimates, or lags, used in defining the spectrum. The proper selection of these quantities will reduce the phenomenon known as "aliasing" which allows power from one frequency to be transferred to another frequency; increase the frequency resolution (or conversely reduce the "smearing" or average effects); or can increase the statistical reliability of the spectral estimates. Proper evaluation of these effects should be made prior to data collection in order that a proper experiment is planned (see references 10 and 11).

RESULTS

Optimum Value Selection

The choice of optimum values of transformer frequency and damping using the peak min. method is reasonably straightforward using curves such as shown in figures 4 and 5. Figure 4 shows that the transformer frequency value of 4.7 cps minimizes the acceleration maximum function for both car locations. (A value of 4.65 cps was used as optimum because it was the value used in the optimizing cycle represented by figures 4, 5 and 6). Figure 5 shows that the transformer damping value of 0.18 minimizes the acceleration maximum function for both car locations. The choice of an optimum value of car damping, however, was not so straightforward. Figure 6 shows that the acceleration maximum function for the end of the car is minimum at a car damping value of 0.057, whereas for the middle of the car the car damping value of 0.114 minimizes the acceleration maximum function. Clearly, no single value of car damping can be chosen that minimizes the acceleration maximum function for both car locations. Therefore, a compromise value must be chosen. Such a compromise value might be chosen several ways. For example, if passengers were to be located only near the middle of the car, and the end of the car used for baggage, then a car damping value of 0.114 would be best. On the other hand, the choice of a car damping value of 0.06 would result in approximately the same value of acceleration maximum function at both car locations. Passengers at both locations would thus receive the same maximum acceleration. A decision on which way to choose the compromise value of car damping was felt to be outside the scope of this study. For the final optimization cycle of this study the car damping value used was $n_s = 0.085$ which is approximately midway between the values minimizing the acceleration at the two car locations.

Transformer Behavior

Curves showing the acceleration maximum function for the transformer are presented in figures 4, 5, and 6 to illustrate the behavior at a system location that was not included in the selection of minimizing values of the parameters. All three figures show that the parameter values minimizing car accelerations do not minimize transformer accelerations. For example, figure 4 shows that at the transformer frequency value of 4.65 cps the transformer acceleration is 50 $^{o}/o$ above its minimum value. This shows, as could have been expected, that optimization of one part of a system can result in non-optimum performance of another part of the system. In the design of a practical system this fact should be taken into account to ensure that all system components including those having non-optimum performance can adequately perform their assigned function.

Sine vs Random Input

The peak minimization method was used to optimize the railroad car model having random displacement inputs as well as sinusoidal input. Curves showing the variation of peak spectral density with transformer frequency, transformer damping and car damping for the final iteration cycle with random inputs were similar in appearance to the curves shown in figures 4, 5 and 6 for the sine input. As an example, figure 9 shows the variation of peak spectral density with car damping for the high estimate random input. Comparison of figure 6 with figure 9 shows the general similarity of the curves for both sine and random input. In particular, the previous discussion concerning the choice of optimum values of the parameters, and the behavior of the transformer applies equally to results for random inputs as well as for sinusoidal input.

The value of transformer frequency obtained as optimum was the same, 4.65 cps., for both random inputs as for the sinusoidal input. The optimum value of transformer damping was 0.18 for both the sinusoidal and the high estimate random input, but was 0.20 for the middle estimate random input. The spectral density maximum function varies by only about 1 °/o between these two values of damping. Therefore, the difference is not considered significant. Comparison of figure 6 with figure 9 shows that the values of car damping that minimize the individual acceleration maximum functions (figure 6) are different from the values that minimize the spectral density maximum functions (figure 9). The values of car damping that minimize the individual maximum functions are presented in Table I for both random inputs and the sine input. Table I shows that the optimum values of damping obtained for each location with the random inputs are at least three times as large as the values obtained with the sinusoidal input. The values of damping obtained with the two random inputs are different by a maximum of about 40 °/o. These large differences in optimum damping values suggest that when railway roughness is expected to be of a random nature, then optimization studies should use random inputs. In addition, the observed variation of optimum damping between the two random inputs, which differ primarily in spectral shape, suggests that the range of spectral shapes to be expected of actual rails should be determined and used in optimization studies.

Peak Min. vs RMS Methods

The variation of rms acceleration at the three locations with transformer damping and frequency is shown in figure 10 and the variation with car damping is shown in figure 11. Figure 10(a) shows that the acceleration at the end of the car is minimum at $f_g = 4.3$ cps while that at the middle of the car is minimum at $f_g = 4.8$. The rms acceleration is not very sensitive to variations of f_g. Therefore, the optimum value of 4.65 cps determined by the peak min. method can be taken as a good compromise value. Figure 10(b) shows that the rms acceleration on the car is insensitive to the value of transformer damping used. Therefore, the value of 0.18 determined by the peak min. method can be used. The rms acceleration was also found to be insensitive to variations of transformer frequency and damping when the middle estimate random input was used, so the values of $f_g = 4.65$ cps and $\eta_g = 0.18$ were suitable values for both input spectra and both optimization methods.

Figure 11 shows that the rms acceleration at each location is minimum for a different value of car damping, and is sensitive to variations of car damping. As previously discussed, considerations outside the scope of this study must be used to determine which value of car damping to use. Values of car damping (from figure 11 and similar results for the middle estimate input) that minimize the acceleration at each car location are presented in table II along with the optimum car damping results previously presented and obtained with the peak min. method. Table II shows that the optimum value of car damping for each location determined by the rms method is about half as large as when determined by the peak min. method. Figure 9 shows that for values of car damping below the optimum for each location the spectral density has a value at the 1 cps peak that is much larger than the values at the 4.5 and 5.5 cps peaks. The acceleration response is thus concentrated near a single frequency. Therefore, if the smaller value of damping obtained by the rms method is chosen to minimize rms acceleration, then the response is concentrated near a single frequency. This may be uncomfortable to passengers. On the other hand, if the higher value of damping is chosen, to minimize the peak value of spectral density, then a higher overall rms acceleration results with the response more evenly spread over the frequency range. In order to choose an optimum value of damping in this situation, the effect on passenger comfort of various acceleration spectral shapes having various rms levels needs to be known. Experience with acoustic noise indicates that both overall rms level and the concentration of energy near a single frequency are important.

CONCLUDING REMARKS

The results of this investigation illustrate some of the considerations required for the use of measured random data in a mathematical study of vibration response minimization. The techniques are illustrated herein by developing specific results for a three-degree-of-freedom mathematical model using a simplified representation of the measured input displacement, however the techniques could be extended to apply to more complex situations.

The specific results obtained from this study of the vertical dynamics of a three-degree-of-freedom model of a railroad car can be summarized as follows.

For some cases, no single value of a parameter to be optimized can be chosen that will minimize the acceleration at all locations on the model. In a practical situation, therefore, the relative importance of the various locations must be determined and preference given in the optimizati i process to the more important locations. An optimization study such as presented herein appears to be valuable to show which system parameters most influence the acceleration at a particular location, to show which locations have minimum accelerations for the same value of the damping or frequency parameters, and to show how sensitive the accelerations are to variations of the system parameters from their optimum values.

The optimum value of one damping parameter obtained when the system input was a random function was different from the value obtained with a sinusoidal input. The optimum value was also different for each of two different spectral shapes of the random input. For the three degree of freedom system studied the differences were large and the accelerations were sensitive to variations of the damping parameter from its optimum value. This result suggests the importance of accurate measurement of the characteristics of the input, in this case the rail irregularities, and the importance of using measured information on the input for optimization studies.

The optimum values of the damping and frequency parameters obtained by two different minimization methods (with the same input characteristics) were different. This result was true for both input spectra used. In particular, when the rms acceleration at a given location was minimized the acceleration response tended to be concentrated near a single frequency, but when the peak value of acceleration spectral density was minimized (spreading the response more evenly over the frequency range) the value of the rms acceleration was increased. In order to choose between the two situations additional information is required about the relative importance to passenger comfort of overall rms acceleration level vs the presence of accelerations concentrated near a single frequency.

REFERENCES

1. Adelson, A.; and Williams, J.: New Metroliner Train Offers Pleasant Ride, But Flying is Faster. The Wall Street Journal, Feb. 27, 1969, p. 1.
2. Anon.: Transportation: Do Fast Trains Have a Real Future? Business Week, Jan. 25, 1969.
3. Lens, W. F.: Vehicle Vibration Analysis Using Frequency Domain Techniques. ASME Paper No. 69-Vibr-66. Trans. ASME.
4. Kaplan, A.; Koval, L. R.; and Choy, F., Jr.: Rail Vehicle Dynamics Analysis for High Speed Ground Transportation Roadbed Study. TRW Systems Report EM-17-22, Sept. 1967.
5. Evensen, D. A.; and Kaplan, A.: Problems of Wheel-Rail Interaction Associated with High-Speed Trains. TRW Systems, Nov. 1967.
6. Hurley, F. J.; Boeser, J. N.; Koch, B. R.; and McConnell, P. J.: Railroad Research Field Testing Program: First Progress Report; Melpar, Inc., for U. S. Dept. of Transportation, Dec. 1968.
7. Pursifull, L. J.; and Prothro, B. E.: Development of a Railroad Roughness Indexing and Simulation Procedure. Shock and Vibration Bull. No. 39, Part 6, March 1969.
8. Law, C. W.: Instrumentation for High-Speed Railroad Research Project. Inst. Soc. Amer. Preprint No. 23-2-TID-67. 22nd Ann. ISA Conf., Sept. 1967.
9. McMunn, J. C.: Multi-Parameter Optimum Damping in Linear Dynamical Systems. PhD Dissertation, University of Minnesota, 1967.
10. Houbolt, J. C.; Steiner, R.; and Pratt, K. G.: Dynamic Response of Airplanes to Atmospheric Turbulence Including Flight Data on Input and Response. NASA TR R-199.
11. Bendat, J. S.; and Piersol, A. G.: Measurement and Analysis of Random Data. Wiley and Sons, New York, 1966.

APPENDIX A

SYMBOLS

$A(t)$	generalized coordinate of beam rigid body mode, $= A_1 \sin\omega t + A_2 \cos\omega t$
$A(0)$	acceleration at end of beam
$A(L/2)$	acceleration at center of beam
$B(t)$	generalized coordinate of beam bending mode, $= B_1 \sin\omega t + B_2 \cos\omega t$
C_g	damping of transformer
C_s	damping of beam
EI	beam bending stiffness
$\overline{EI} = \pi^6 EI/8L^3$	
$g(t)$	displacement of transformer mass
G	acceleration of gravity
k_g	spring constant of transformer
k_s	spring constant of beam support
L	beam length, 85 ft.
M	beam mass, 153,600/G, lbs-sec^2/ft
M_g	transformer mass, 13,000/G, lbs-sec^2/ft
n_g	transformer damping coefficient, $= C_g/2 M_g \omega_g$
n_s	beam damping coefficient, $= C_s/M\omega_s$
S_o	amplitudes of applied displacement
$S(\omega)$	spectral density of applied displacement
t	time
$w(x,t)$	beam displacement, $= A(t) + B(t)\left[1-\pi(\sin \pi x/L)/2\right]$
x	distance along beam

$\zeta \quad = 1 - \pi\left[\sin 12.5\,\pi/85\right]/2$

ω circular frequency of applied displacement

$f_B = \frac{\omega_B}{2\pi}$ beam bending frequency, $f_B = \sqrt{\pi^4 EI/8ML^3} = 5$ cps

$f_g = \frac{\omega_g}{2\pi}$ transformer frequency, $= \sqrt{k_g/M_g}\,/2\pi$

$f_s = \frac{\omega_s}{2\pi}$ beam rigid body frequency, $f_s = \sqrt{2k_s/M}\,/2\pi = 1$ cps

APPENDIX B

EQUATIONS

The three degrees of freedom assumed for the mathematical model shown in figure 2 were rigid body translation of the beam, the first bending mode of the beam and the translation of the transformer. The displacement input was $S_O \sin \omega t$ at both ends of the beam, so only symmetrical motions were excited. The equations of motion for this three degree of freedom mathematical model are:

$$\begin{bmatrix} M & 0 & 0 \\ 0 & M(\frac{\pi^2}{8} - 1) & 0 \\ 0 & 0 & M_g \end{bmatrix} \begin{Bmatrix} \ddot{A} \\ \ddot{B} \\ \ddot{g} \end{Bmatrix} + \begin{bmatrix} 2C_s + C_g & 2C_s\zeta + C_g(1 - \frac{\pi}{2}) & -C_g \\ 2C_s\zeta + C_g(1 - \frac{\pi}{2}) & 2C_s\zeta^2 + C_g(1 - \frac{\pi}{2})^2 & -C_g(1 - \frac{\pi}{2}) \\ -C_g & -C_g(1 - \frac{\pi}{2}) & C_g \end{bmatrix} \begin{Bmatrix} \dot{A} \\ \dot{B} \\ \dot{g} \end{Bmatrix}$$

$$+ \begin{bmatrix} 2k_s + k_g & 2k_s\zeta + k_g(1 - \frac{\pi}{2}) & -k_g \\ 2k_s\zeta + k_g(1 - \frac{\pi}{2}) & 2k_s\zeta^2 + k_g(1 - \frac{\pi}{2})^2 + \overline{EI} & -k_g(1 - \frac{\pi}{2}) \\ -k_g & -k_g(1 - \frac{\pi}{2}) & k_g \end{bmatrix} \begin{Bmatrix} A \\ B \\ g \end{Bmatrix} = \begin{Bmatrix} 2k_s \\ 2k_s\zeta \\ 0 \end{Bmatrix} S_o \sin\omega t$$

$$+ \begin{Bmatrix} 2C_s\omega \\ 2C_s\omega\zeta \\ 0 \end{Bmatrix} S_o \cos\omega t$$

These equations were divided by MS_o , and written in terms of the matrices $\overline{M}$, $\overline{K}$ and $\overline{C}$, the generalized coordinates

$$\{q\} = \begin{Bmatrix} A/S_o \\ B/S_o \\ g/S_o \end{Bmatrix} ,$$

and the force vectors

$$S_1 = \begin{Bmatrix} \omega_s^{\ 2} \\ \zeta\omega_s^{\ 2} \\ 0 \end{Bmatrix} , \quad S_2 = \begin{Bmatrix} 2n_s\omega_s \\ 2n_s\omega_s\zeta \\ 0 \end{Bmatrix} ,$$

as:

$$\overline{M}\ddot{q} + \overline{C}\dot{q} + \overline{K}q = S_1 \sin\omega t + S_2 \cos\omega t \tag{B1}$$

The steady state part of the solution is then taken as:

$$q = q_1 \sin\omega t + q_2 \cos\omega t$$

where:

$$q_1 = \begin{Bmatrix} A_1/S_o \\ B_1/S_o \\ g_1/S_o \end{Bmatrix} , \quad q_2 = \begin{Bmatrix} A_2/S_o \\ B_2/S_o \\ g_2/S_o \end{Bmatrix}$$

which when substituted into equation (B1) gives:

$$-\omega^2\overline{M}\sin\omega t\; q_1 - \omega^2\overline{M}\cos\omega t\; q_2 + \omega\overline{C}\cos\omega t\; q_1 - \omega\overline{C}\sin\omega t\; q_2$$

$$+ \overline{K}\sin\omega t\; q_1 + \overline{K}\cos\omega t\; q_2 = S_1\sin\omega t + S_2\cos\omega t$$

Equating coefficient of $\sin\omega t$ and $\cos\omega t$ leads to the 6 equations of motion:

$$\begin{bmatrix} \overline{K} - \omega^2\overline{M} & -\omega\overline{C} \\ \omega\overline{C} & \overline{K}-\omega^2\overline{M} \end{bmatrix} \begin{Bmatrix} q_1 \\ q_2 \end{Bmatrix} = \begin{Bmatrix} S_1 \\ \omega S_2 \end{Bmatrix} \qquad \text{(B2)}$$

The elements of the mass ($\overline{M}$), damping ($\overline{C}$) and stiffness ($\overline{K}$) matrices in equation (B2) are:

$$M_{11} = 1$$

$$M_{22} = \frac{\pi^2}{8} - 1$$

$$M_{33} = M_g/M = m_g$$

All other M_{ij} are equal to zero.

$$K_{11} = \omega_s^2 + m_g\omega_g^2$$

$$K_{12} = K_{21} = \zeta\omega_s^2 + (1 - \pi/2)m_g\omega_g^2$$

$$K_{13} = K_{31} = -m_g\omega_g^2$$

$$K_{22} = \zeta^2\omega_s^2 + (1 - \pi/2)^2 m_g\omega_g^2 + \omega_B^2/4$$

$$K_{23} = K_{32} = -(1 - \pi/2)m_g\omega_g^2$$

$$K_{33} = m_g\omega_g^2$$

$$C_{11} = 2n_s\omega_s + 2n_g m_g\omega_g$$

$$C_{12} = C_{21} = 2n_s\omega_s\zeta + 2n_g\omega_g m_g(1 - \pi/2)$$

$$C_{13} = C_{31} = -2n_g m_g\omega_g$$

$$C_{22} = 2n_s\omega_s\zeta^2 + 2n_g\omega_g m_g(1 - \pi/2)^2$$

$$C_{23} = C_{32} = -2n_g\omega_g m_g(1 - \pi/2)$$

$$C_{33} = 2n_g\omega_g m_g$$

Values of the column vectors q_1 and q_2 obtained from equations (B2) were then used to obtain the acceleration transfer functions from the equations:

$$\frac{A(L/2)}{GS_o} = \left\{\left[A_1 + B_1(1 - \pi/2)\right]^2 + \left[A_2 + B_2(1 - \pi/2)\right]^2\right\}^{1/2} \omega^2/S_oG \qquad \text{(B3)}$$

$$\frac{A(0)}{GS_o} = \left\{\left[A_1 + B_1\right]^2 + \left[A_2 + B_2\right]^2\right\}^{1/2} \omega^2/S_oG \qquad \text{(B4)}$$

$$\frac{\ddot{\varepsilon}}{GS_o} = (\varepsilon_1{}^2 + \varepsilon_2{}^2)^{1/2} \omega^2/S_oG \qquad (B5)$$

The spectral density and rms values of the accelerations were found from:

$$S_{L/2}(\omega) = \left[A(L/2)/GS_o\right]^2 S(\omega) \qquad (B6)$$

$$A_{rms}(L/2) = \left[\int_o^{\infty} S_{L/2}(\omega)\, d\omega\right]^{1/2} \qquad (B7)$$

TABLE I. - OPTIMUM VALUES OF CAR DAMPING.

Location \ Input	Sine	High Random	Middle Random
	Car damping, n_s =		
Middle of car	.114	.35	.51
End of car	.057	.20	.28
Transformer	.047	.17	.23

TABLE II. - OPTIMUM CAR DAMPING FROM TWO METHODS.

	High Random Input		Middle Random Input	
Location \ Optimization method	Peak-min.	RMS	Peak-min.	RMS
	Car damping, n_s =			
Middle of car	.35	.175	.51	.23
End of car	.20	.09	.28	.13
Transformer	.17	.10	.23	.14

Figure 1.- "Metroliner" high-speed train.

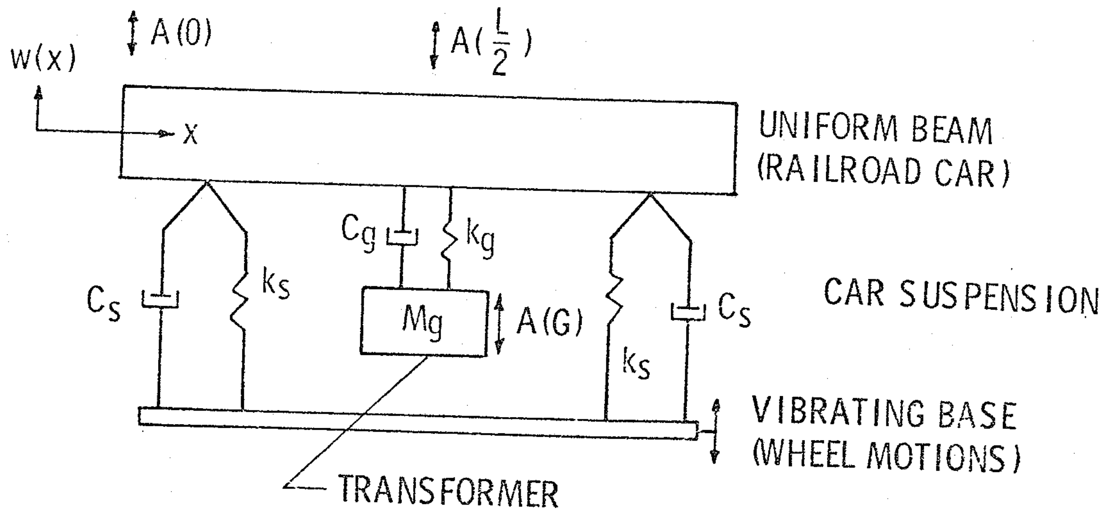

	CAR	TRANSFORMER
WEIGHT, lbs	153,600	13,000
FREQUENCY, cps	1, 5	f_g, VARIED
DAMPING	n_s, VARIED	n_g, VARIED

Figure 2.- Railroad car vibration model.

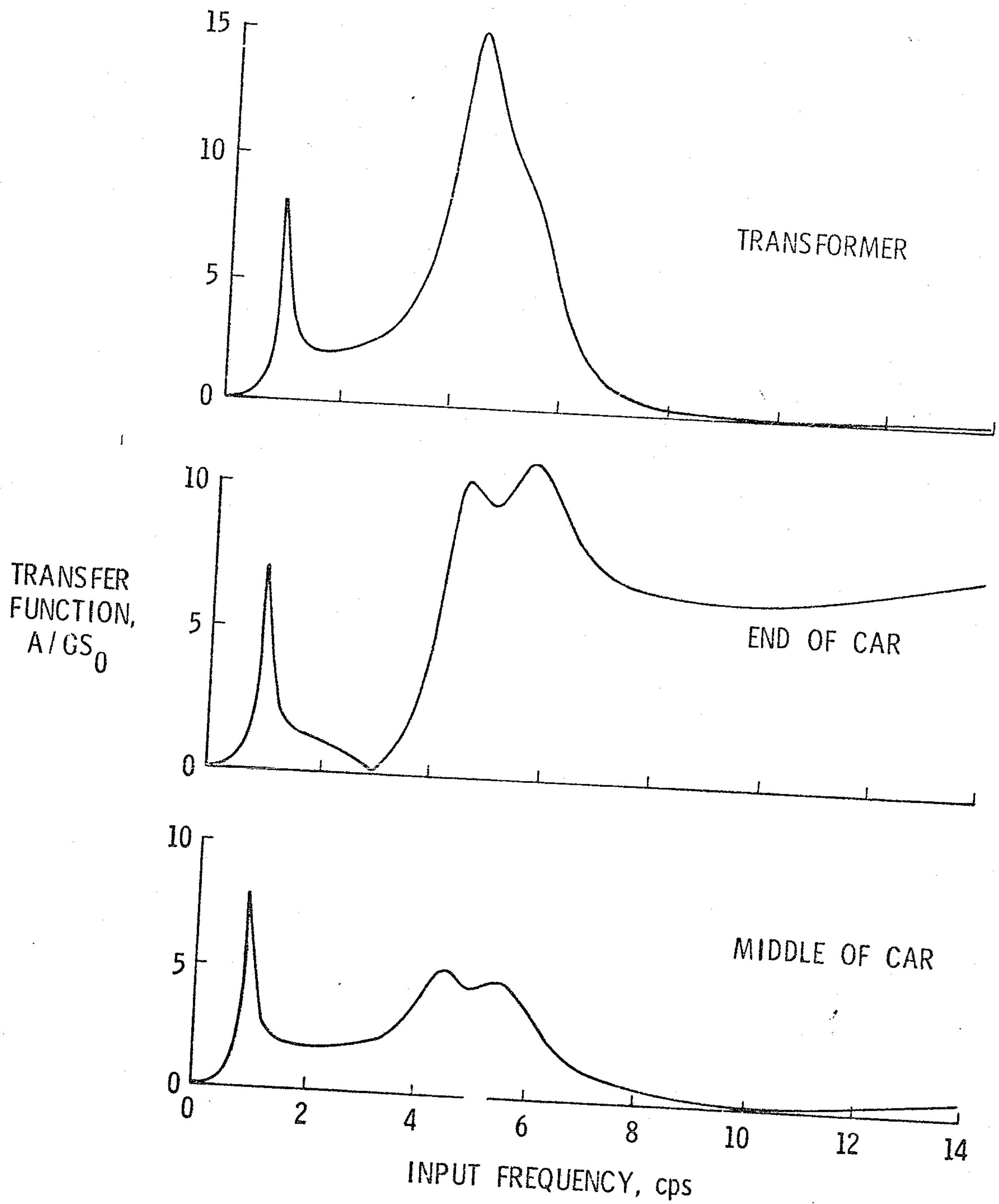

Figure 3.- Acceleration transfer functions. Sine input, $f_g = 4.65$ cps, $n_g = 0.18$, $n_s = 0.085$.

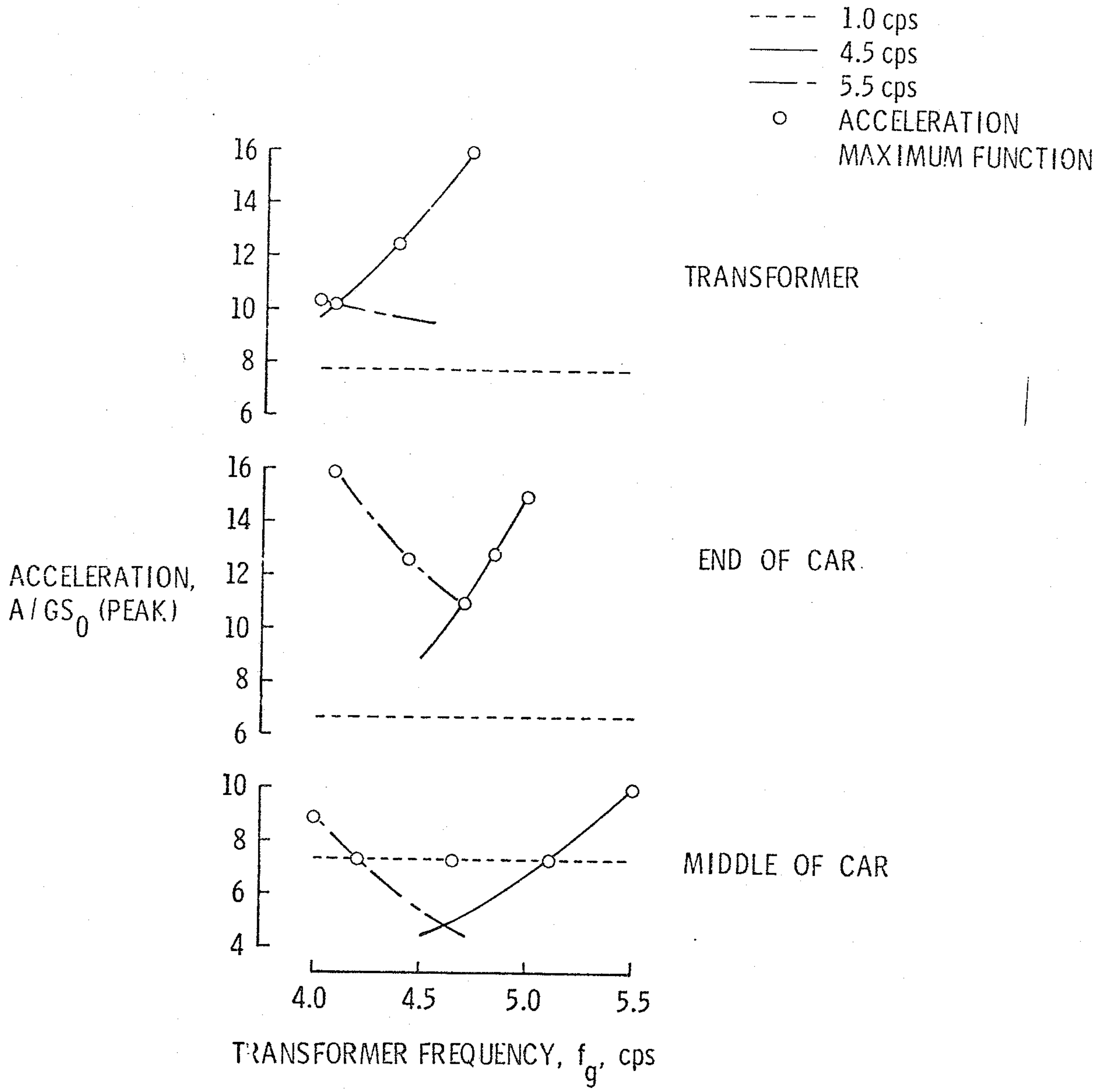

Figure 4.- Variation of peak of acceleration transfer function with transformer frequency. Sine input, $n_g = 0.18$, $n_s = 0.085$.

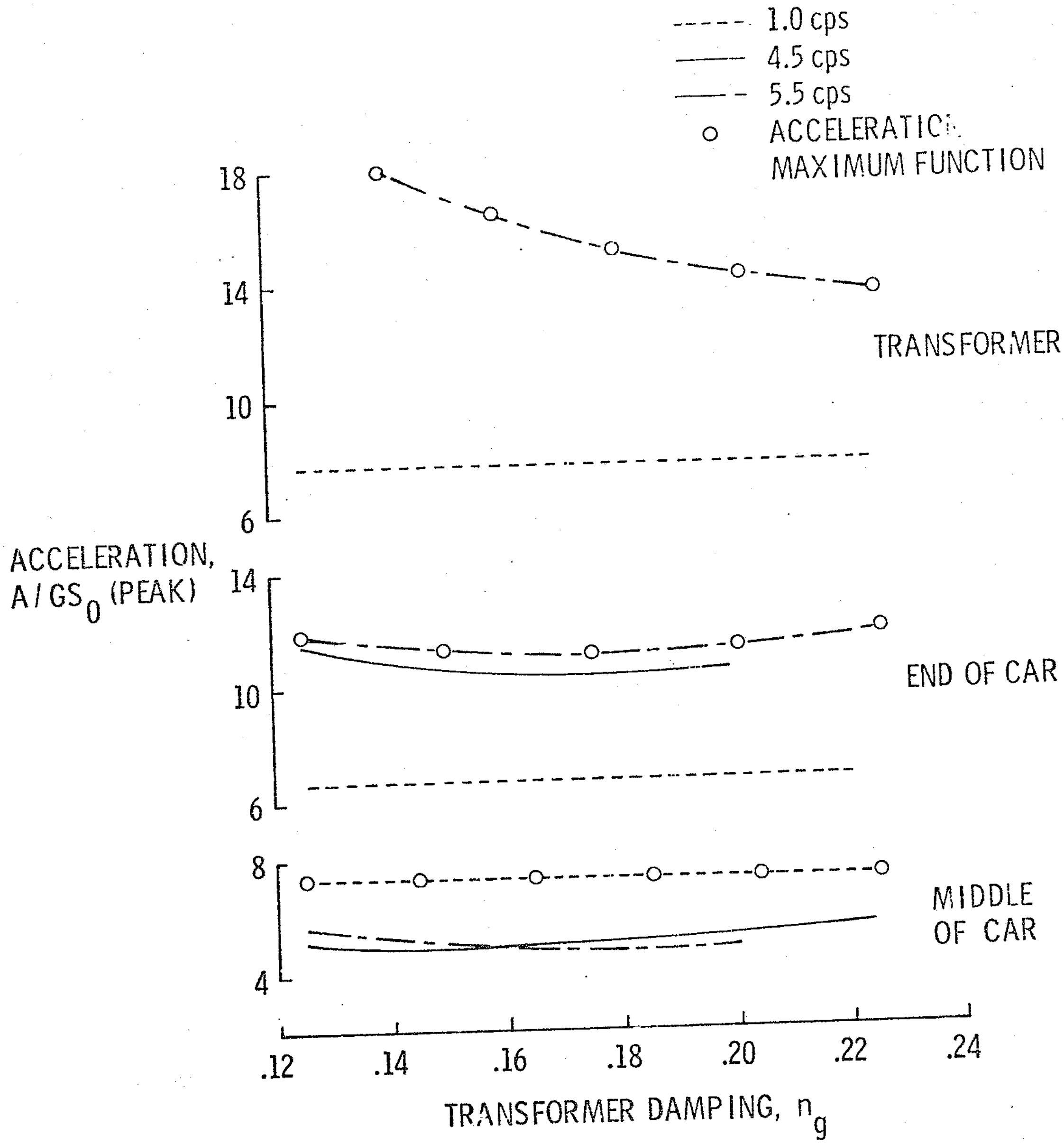

Figure 5.- Variation of peak of acceleration transfer function with transformer damping. Sine input, f_g = 4.65 cps, n_s = 0.085.

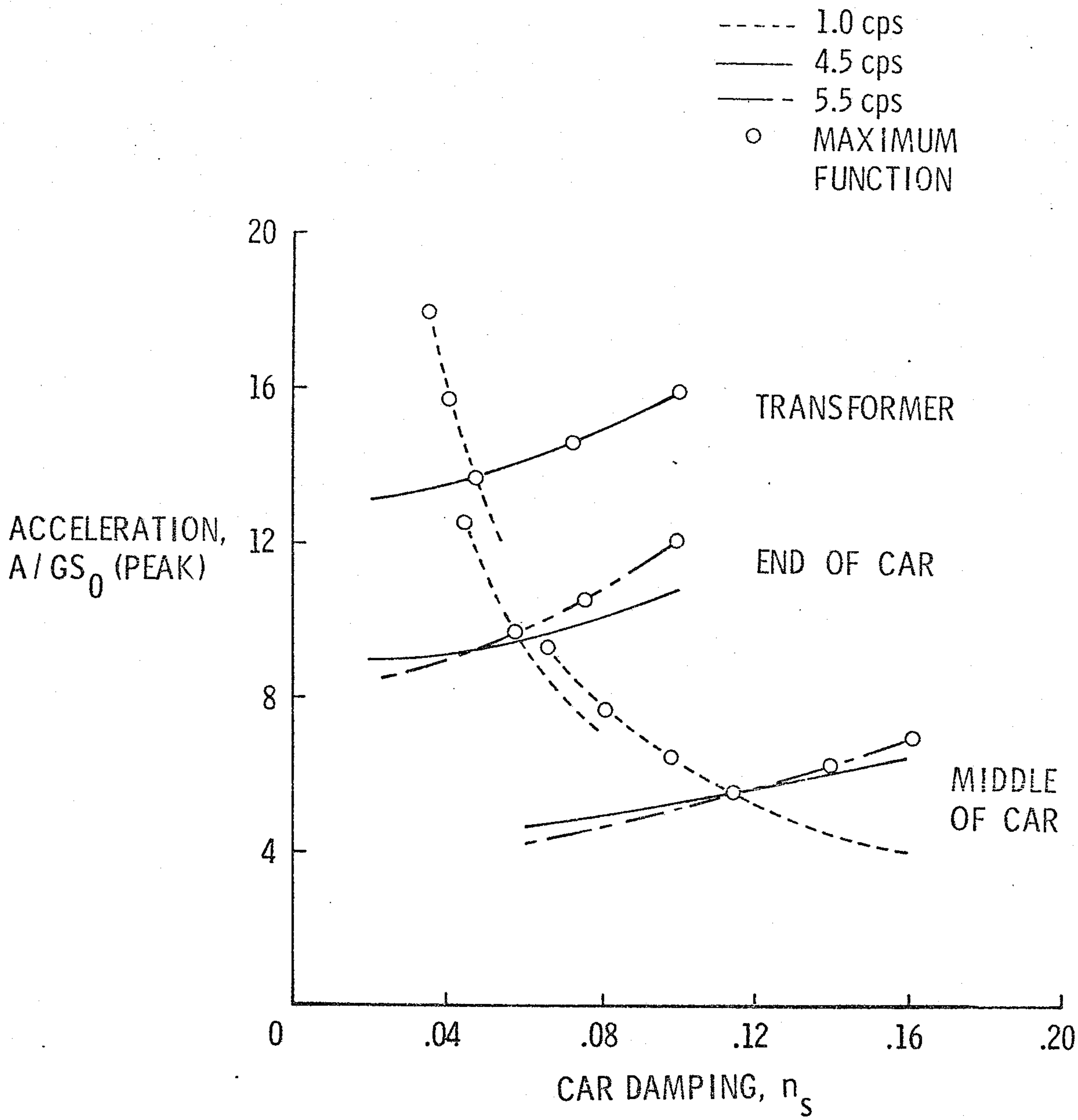

Figure 6.- Variation of peak of acceleration transfer function with car damping. Sine input, f_g = 4.65 cps, n_g = 0.18.

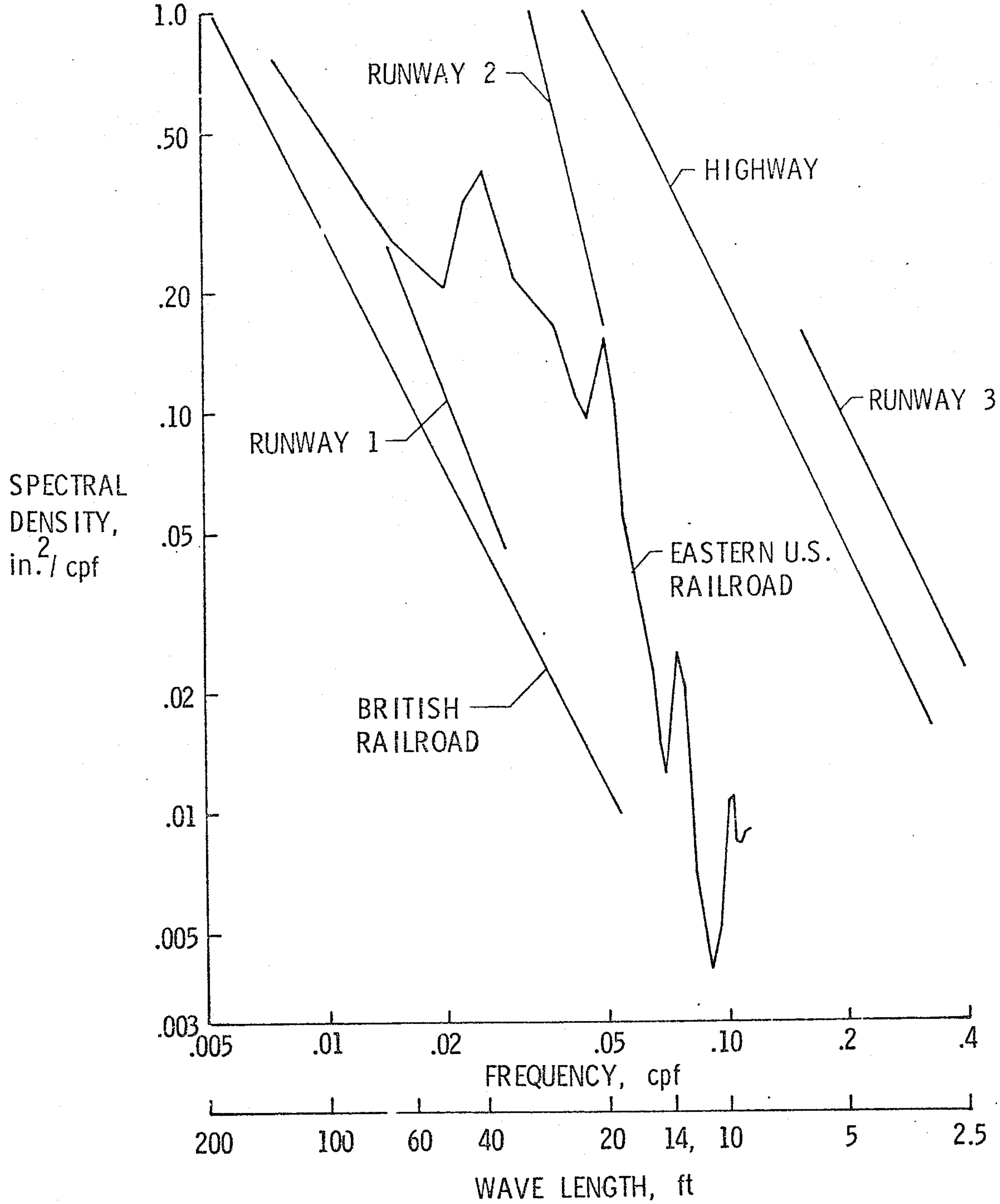

Figure 7.- Measured spectral density of typical transportation surfaces.

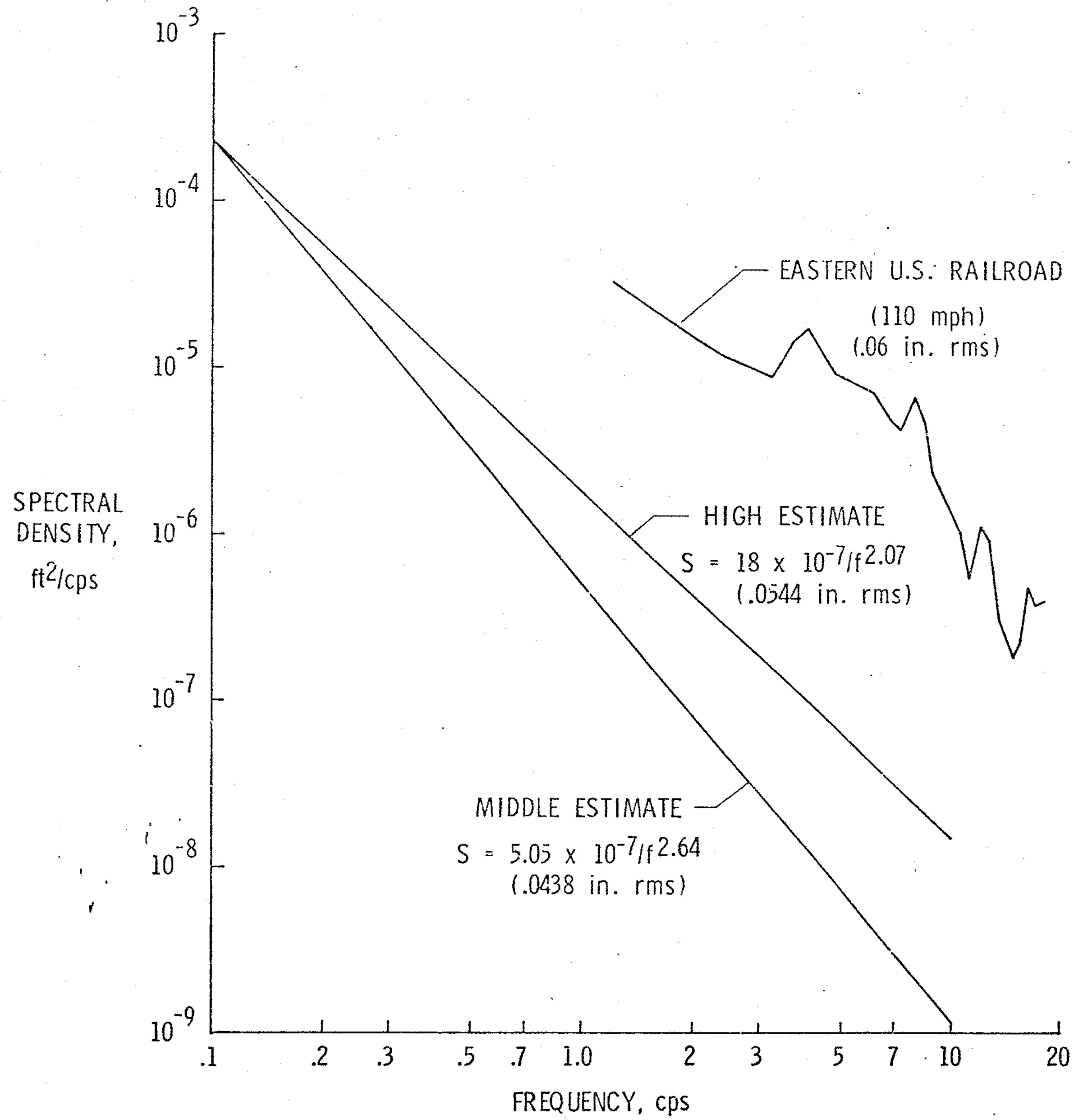

Figure 8.- Spectral density estimates for input to mathematical model.

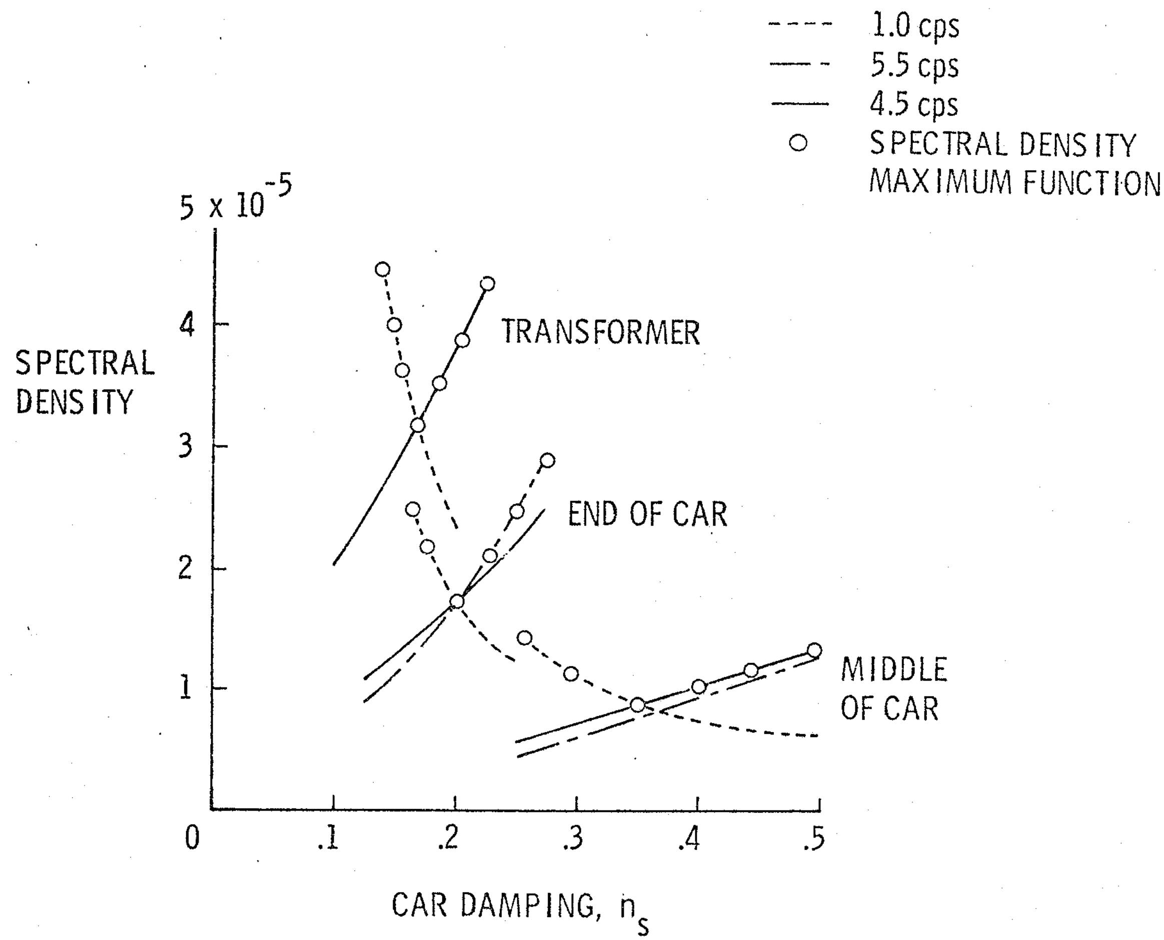

Figure 9.- Variation with car damping of the peak value of spectral density. High estimate input, f_g = 4.65 cps, η_g = 0.18.

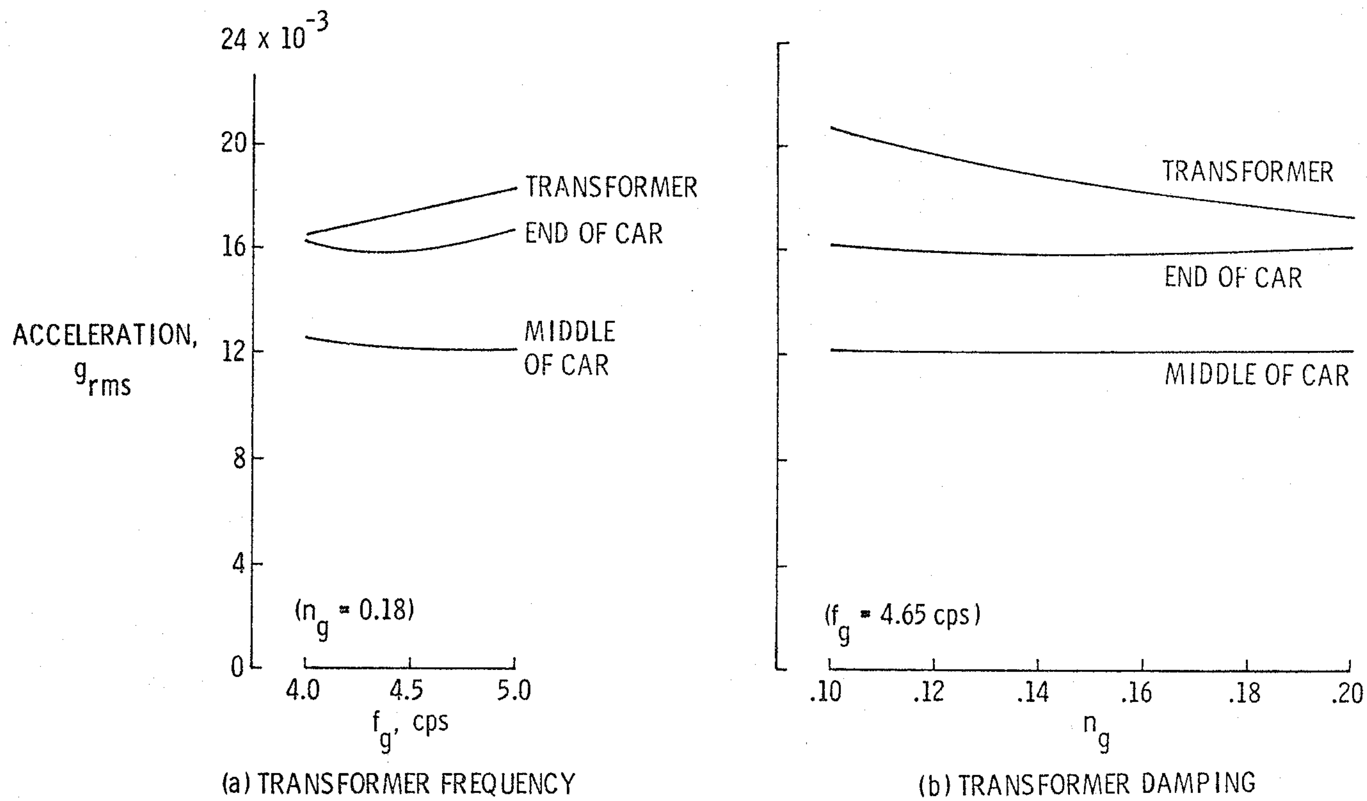

Figure 10.- Variation of rms acceleration with transformer frequency and damping. High estimate input, $n_s = 0.12$.

NASA-Langley, 1969

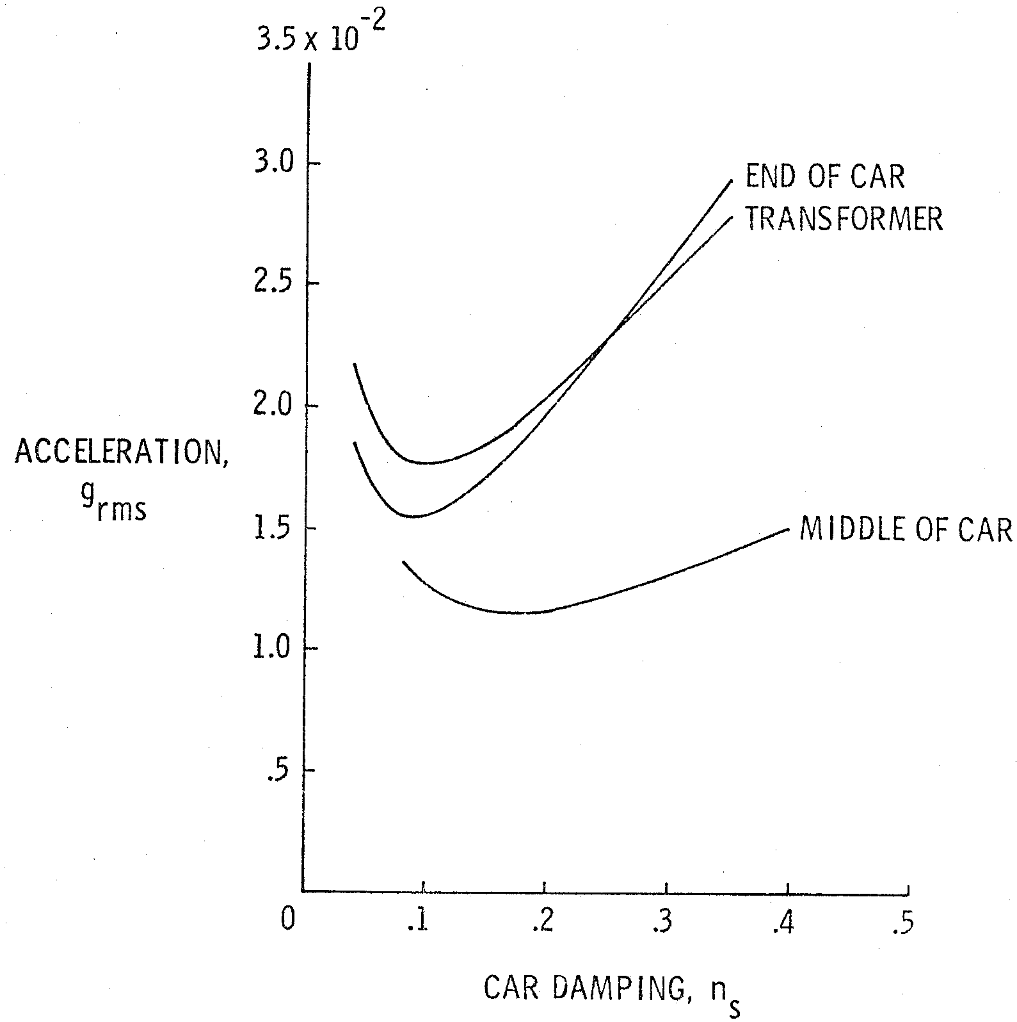

Figure 11.- Variation of rms acceleration with car damping. High estimate input, $f_g = 4.65$ cps, $n_g = 0.18$.